View metadata, citation and similar papers at core.ac.uk
brought to you by CORE
provided by Repositorio da Universidade da Coruña

Neuron, vol. 36, (5): 969-978

Synaptic Integration by V1 Neurons Depends on Location within the Orientation Map

James Schummers, Jorge Mariño, Mriganka Sur

Abstract
Neurons in the primary visual cortex (V1) are organized into an orientation map consisting of orientation domains arranged radially around “pinwheel centers” at which the representations of all orientations converge. We have combined optical imaging of intrinsic signals with intracellular recordings to estimate the subthreshold inputs and spike outputs of neurons located near pinwheel centers or in orientation domains. We find that neurons near pinwheel centers have subthreshold responses to all stimulus orientations but spike responses to only a narrow range of orientations. Across the map, the selectivity of inputs covaries with the selectivity of orientations in the local cortical network, while the selectivity of spike outputs does not. Thus, the input-output transformation performed by V1 neurons is powerfully influenced by the local structure of the orientation map.

Introduction

Primary visual cortex (V1) is the first level in the visual pathway in which neurons show pronounced selectivity for the orientation of a visual stimulus (Hubel and Wiesel, 1962). V1 neurons receive feedforward excitatory inputs, local intracortical excitatory and inhibitory inputs, as well as long-range connections. Understanding how V1 neurons integrate these varied sources of synaptic input to generate responses is an important step in understanding information processing in visual cortex. Numerous studies suggest that inputs from intracortical networks may have profound effects on visual responses, particularly with regard to orientation selectivity Gilbert and Wiesel 1990, Crook et al. 1991, Knierim and van Essen 1992, Crook et al. 1997, Levitt and Lund 1997, Toth et al. 1997, Dragoi et al. 2000, Schuett et al. 2001 and Yao and Dan 2001.

The orientation preference map in V1 affords an opportunity to address the role of the local cortical network in shaping responses. Orientation columns are arranged in a map with a radial, “pinwheel” configuration Bonhoeffer and Grinvald 1991 and Blasdel 1992. That is, neurons sharing a similar orientation preference are grouped together in “orientation domains,” across which preferred orientation changes slowly and continuously, that are arranged radially around pinwheel centers at which the representation of all orientations converge. Despite this diversity in the local structure of the functional map, available data suggest that the extent of local connections is relatively uniform across the orientation map Malach et al. 1993 and Yousef et al. 2001. Thus, it is likely that the functional connectivity within the local cortical circuit varies considerably between locations in the orientation map such that near pinwheel centers, neurons have local connections with neurons having a wide range of orientation preferences (Das and Gilbert, 1999), whereas far from pinwheel centers, connectivity is restricted to neurons sharing similar orientation preferences. Few studies to date have incorporated information about the heterogeneous local structure of the orientation map, which would predict heterogeneity in the cortical inputs to V1 neurons (though see McLaughlin et al. 2000, Dragoi et al. 2001 and Wielaard et al. 2001).

In fact, there exist clues in the literature that there may indeed be substantial diversity in both the excitatory and inhibitory inputs that single V1 neurons receive. Simple cells in thalamic-recipient layers have receptive fields that appear to be constructed by excitation from aligned thalamic inputs Chapman et al. 1991, Reid and Alonso 1995 and Lampl et al. 2001, and for many cells, excitation and inhibition are both strongest at the preferred orientation Ferster 1986 and Anderson et al. 2000a. However, other experiments have shown that inhibition can be stronger at nonoptimal, including orthogonal, orientations (Volgushev et al., 1993; see also Anderson et al., 2000a). Analysis of the dynamics of responses to rapidly flashed bars (Volgushev et al., 1995) or gratings Ringach et al. 1997, Ringach et al. 2002 and Gillespie et al. 2001 has also shown diversity in the magnitude and timing of hyperpolarization and depolarization of the membrane potential, and in the enhancement and suppression of spike

responses. Furthermore, analysis of the contribution of the spike threshold to orientation tuning has shown that the degree to which this nonlinearity sharpens selectivity varies considerably across the population Carandini and Ferster 2000 and Volgushev et al. 2000 and is influenced by the temporal structure of the membrane potential during optimal and nonoptimal stimulation (Volgushev et al., 2002). One possible reason for the diversity of excitatory and inhibitory inputs to neurons may be the laminar location of cells and the recoding of orientation in different laminae (Martinez et al., 2002). Here, we asked whether another powerful source of input diversity, the orientation composition of the local cortical network created by the pinwheel structure of the orientation map, influences synaptic integration by V1 neurons.

Results

We have recorded intracellularly from neurons at known locations in the orientation map in order to estimate the orientation selectivity of both the inputs to, and outputs of, individual V1 neurons. We targeted penetrations to either pinwheel centers or far from them, close to the centers of orientation domains. Our aim was to evaluate the selectivity of subthreshold and spike responses as a function of map location.

Figure 1 shows an example of our recordings and the extraction of parameters used in the subsequent analysis. Figure 1A shows six trials of the raw membrane potential during the presentation of a drifting grating of preferred orientation and direction. Figure 1B shows the average membrane potential after the spikes have been removed, the individual trials have been averaged, and the trace has been smoothed. The average potential of the trace during the grating, minus the resting potential, is termed the membrane potential response. Figure 1C shows the peristimulus time histogram (PSTH) of the average firing rate, from which the spike response (average minus spontaneous) is extracted. All subsequent analyses were performed on the membrane potential response and spike response by measuring their magnitude as a function of stimulus orientation.

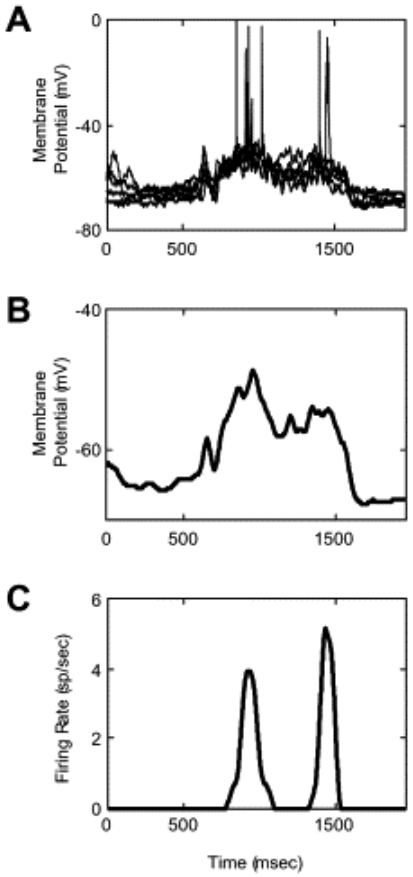

Figure 1. Representative Example of Intracellular Recording and Extraction of Response Parameters
(A) Six traces of raw membrane potential in response to a drifting grating stimulus. Some action potentials are chopped due to sampling frequency; in fact, the action potentials overshot zero. The stimulus was turned on at 500 ms and turned off at 1500 ms.
(B) Average membrane potential after the spikes were removed by interpolation, the six trials were averaged, and the trace was smoothed with a sliding boxcar. The difference between the average membrane potential during the stimulus period minus the resting potential (membrane potential during blank stimulus or before stimulus appearance) is extracted and termed the membrane potential response. In this case, the response is 10mV.
(C) PSTH of the average rate of the spikes extracted from (A). As in (B), the spike response is extracted by subtracting the baseline from the average across the entire stimulus period, in this case, 2 spikes/s.

Figure 2 shows the responses of a simple cell and a complex cell that are typical of those found far from pinwheel centers, in orientation domains. The simple cell in Figures 2A–2D shows a large depolarization to a narrow range of stimulus orientations and a spike response to a similarly narrow range of orientations. Because simple cell responses follow the luminance modulation of a drifting grating stimulus Movshon et al. 1978 and Skottun et al. 1991, we have plotted separately the mean response and the temporal modulation of the response with each cycle of the grating (Figures 2C and 2D). The membrane potential shows a strong, mostly depolarizing response to each phase of the grating of optimal or near-optimal orientation. The modulations of the membrane potential ride on a small baseline depolarization that is also orientation selective. Stimuli progressively away from the preferred orientation lead to responses that show progressively less modulation and reduced net depolarization. Thus, the tuning curves for both the mean membrane potential and spike responses (Figure 2C), and of the temporal modulation of these responses (Figure 2D), are narrowly tuned, and responses fall to zero for stimuli orthogonal to the optimal. Figures 2E–2G show the responses of a complex cell, also recorded within an orientation domain. As is typical of complex cells (Skottun et al., 1991), the cell does not show temporal modulation of its response to each phase of the drifting grating but instead a general elevation in response to gratings at and near its preferred orientation. Again, this cell shows strong depolarization and spike responses only near its preferred orientation, with no significant response to the orthogonal orientation. Thus, both simple and complex cells located in orientation domains show a strong membrane potential response only for a limited range of stimulus orientations, and this selectivity is reflected in their spike responses.

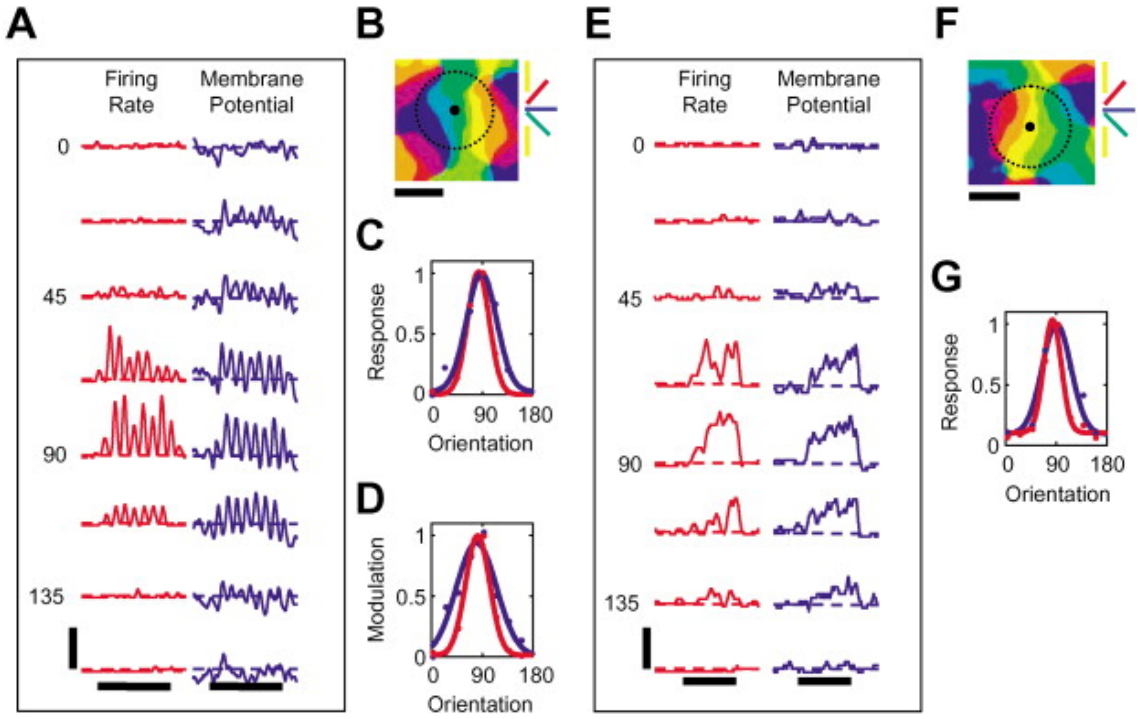

Figure 2. Responses of a Simple and a Complex Cell Recorded in Orientation Domains

(A) The responses of a simple cell recorded at the location marked by the dot in the orientation angle map (shown in [B]). The spike response (left column) and membrane potential response (right column) of the neuron to drifting gratings of eight orientations spanning 180° are shown. In this figure and in subsequent figures, red is used to represent spike (firing rate) responses, whereas blue is used to represent membrane potential responses. Each trace is the average of five repetitions of a grating stimulus, with the orientation shown to the left of the trace. The dashed red and blue lines represent the average resting spike rate and membrane potential, respectively. The black bars below the bottom traces show the time of the grating stimulus. The vertical scale bar represents 8 spikes/s or 10mV; the horizontal scale bars represent 2 s.

(B) Orientation angle map taken from the region of cortex surrounding the recording site. The color of each pixel codes for the optimal orientation at that pixel, as indicated in the color bars at the top right. The same color code applies to all orientation maps shown throughout. The dotted circle denotes a local region of the map of radius 400 μm centered on the recorded cell (see text for details). The scale bar here and in subsequent figures represents 0.5 mm.

(C) Tuning curves of the amplitude of membrane potential (blue) and spike (red) responses, taken as the average across the duration of the stimulus presentation (the F0 component of the response). Here, and in subsequent examples, the lines correspond to a gaussian estimate of the tuning curve that was fit to the data points, shown as small circles. The responses to a uniform gray screen of the same mean luminance as the grating stimulus were defined as baseline and were subtracted from the average firing rate and membrane responses. All tuning curves are normalized and aligned to 90° for ease of comparison.

(D) Tuning curves of the amplitude of modulation in response to each phase of the stimulus grating (the F1 component of the response).

(E and F) Spike and membrane potential responses (E) of a complex cell recorded in an orientation domain (as shown in [F]). The vertical scale bar represents 8 spikes/s or 10mV; the horizontal scale bars represent 2 s.

(G) Tuning curves of the average amplitude of the spike and membrane potential responses.

Figure 3 demonstrates responses from a simple cell and a complex cell that are typical of cells near pinwheel centers. These neurons demonstrate strikingly different profiles of subthreshold responses compared to neurons in orientation domains. The simple cell shown in Figures 3A–3D has a robust depolarization to all orientations. The temporally modulated component of the membrane potential is narrowly tuned (Figure 3D), most likely due to the receptive field structure of simple cells. The response modulation rides on a relatively large baseline depolarization, which is prominent at all stimulus orientations, including those orthogonal to the preferred orientation. The mean depolarization to the orthogonal orientation is roughly half as large as that to the preferred orientation, and thus the tuning curve of the membrane potential response has a large offset (Figure 3C). This behavior was seen in several simple cells found near pinwheel centers and may result from spatial phase-insensitive inputs arising from other neurons in the local network. The spike response of the cell generally follows the modulated component of the membrane potential, largely ignoring its baseline component, and is therefore sharply tuned for orientation. The complex cell in Figures 3E–3G also shows a depolarization in response to all stimulus orientations. Similar to the simple cell of Figure 3C, the membrane potential tuning curve of this neuron (Figure 3G) has a large offset in that an orthogonal stimulus evokes a

depolarization that is nearly half the amplitude of the response to the preferred stimulus. The spike tuning curve has a much smaller offset, indicating that nonpreferred stimuli evoke little spiking activity. It is noteworthy that the spike responses of these pinwheel neurons do not follow the membrane potential particularly faithfully. This may be the result of averaging several repetitions of the stimulus (Anderson et al., 2000b) or of differences in the temporal microstructure of the fluctuations in membrane potential for different stimulus orientations, which has recently been shown to dramatically affect spike generation in visual cortical neurons (Volgushev et al., 2002). Regardless of the mechanism, these cells generate significantly more spikes for the preferred orientation, despite relatively similar average depolarizations in response to several orientations. Thus, these examples indicate that both simple and complex cells located near pinwheel centers receive synaptic inputs over a broad range of stimulus orientations, although not all of these inputs are represented in the spike outputs.

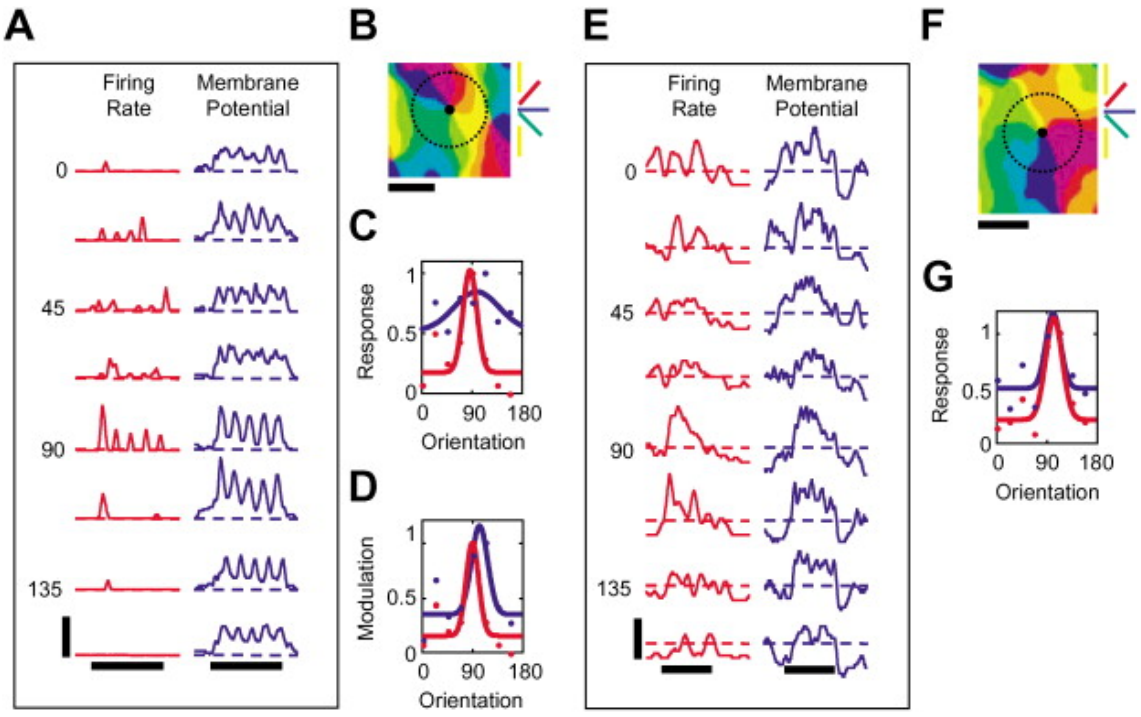

Figure 3. Responses of a Simple and a Complex Cell Recorded Near Pinwheel Centers
(A–D) Responses of a simple cell recorded at the location marked by the dot in the orientation angle map (shown in [B]). The vertical scale bar represents 3 spikes/s or 8mV; horizontal scale bars represent 2 s. All conventions in (A)–(D) are the same as in Figure 2.
(E–G) Responses of a complex cell recorded at a pinwheel center (as shown in [F]). The vertical scale bar represents 5 spikes/s or 7mV; horizontal scale bars represent 1 s. All conventions in (E)–(G) are the same as in Figure 2.

Our population includes a total of 27 cells, including 15 in orientation domains (4 simple and 11 complex) and 12 near pinwheel centers (5 simple and 7 complex). Neurons were sampled across all layers; the distributions of recording depths were similar between the pinwheel and orientation domain cell groups (data not shown). Across the population, we consistently found a difference between the orientation selectivity of the membrane potential responses in neurons located in orientation domains and those near pinwheel centers. The average tuning curves of the spike rate are indistinguishable between pinwheel cells and orientation domain cells (Figure 4A), as described previously Maldonado et al. 1997 and Dragoi et al. 2001. However, the average tuning curves of the membrane potential responses are clearly different (Figure 4B); the tuning curve of the pinwheel cells is shallower, with a larger offset, than that of the orientation domain cells. To enable quantitative comparisons of tuning between the two populations, we calculated three indices of orientation selectivity (Experimental Procedures). A two-factor ANOVA of map location (pinwheel versus domain) and cell type (simple versus complex) on the orientation selectivity index (OSI) indicates a main effect of map location ($F(1,23) = 4.68$, $p < 0.05$) but no effect of cell type ($F(1,23) = 0.92$, $p > 0.3$). Given this result, simple and complex cells have been grouped together for all subsequent analyses. A comparison of the OSI (Figure 4C) reveals that whereas

the distribution of firing rate OSIs is similar between the two groups ($p > 0.4$), the membrane potential OSIs are significantly lower in the pinwheel population ($p < 0.03$). A comparison of the modulation index (MI; Figure 4D) also shows that the values for spike responses are similar ($p > 0.1$) whereas the values for membrane potential responses are significantly lower in the pinwheel neurons ($p < 0.03$). However, the distributions of tuning curve half-widths (data not shown) are not statistically different between neurons at pinwheel centers and orientation domains for either the spike rate ($p > 0.9$) or the membrane potential response ($p > 0.4$). Thus, these quantitative comparisons confirm the impression from the average tuning curves that the difference between the two populations of neurons is not in the responses at and around the preferred orientation (as measured by the half-width), but rather lies in whether the full range of stimulus orientations drives synaptic inputs to the cell (as measured by the OSI) and particularly whether orthogonal stimuli evoke larger subthreshold depolarizations in pinwheel neurons (as reflected in the MI).

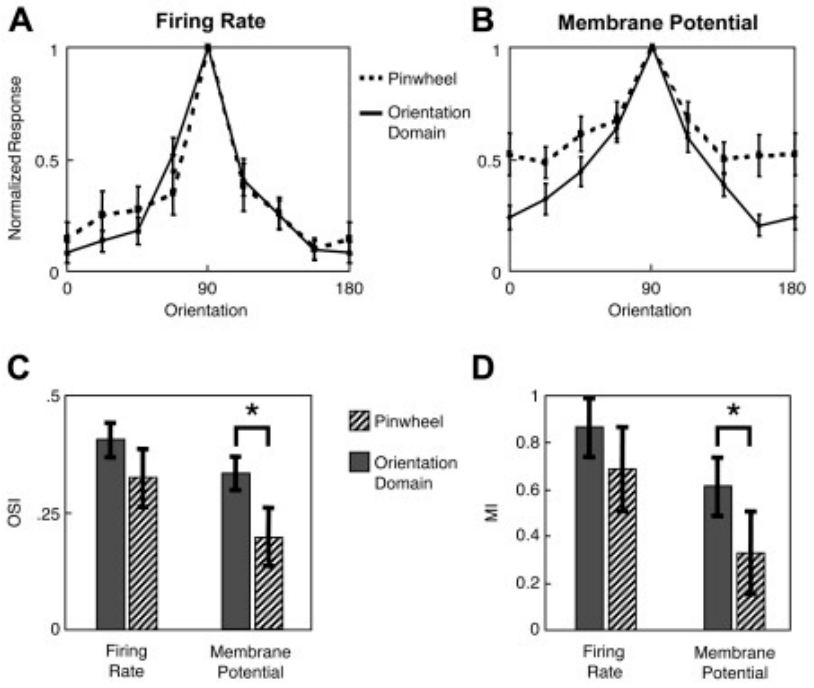

Figure 4. Pinwheel Cells Have Less Selective Inputs across Our Population of Cells
(A) Average tuning curves (±SEM) of the firing rate responses for our sample of pinwheel neurons (n = 12) and orientation domain neurons (n = 15). Tuning curves were normalized, and aligned to the peak response before averaging.
(B) Average tuning curves of the membrane potential responses of the same pinwheel and orientation domain neurons. Curves were normalized, and aligned to the peak response.
(C and D) Bar plots showing the average values of the orientation selectivity index (OSI) and modulation index (MI) of the firing rate and membrane potential tuning curves from the population of neurons grouped according to recording location (orientation domain or pinwheel). "*" represents a statistically significant difference of population means (Student's t test; $p < 0.05$).

The orientation map does not consist only of neurons in pinwheel centers and orientation domains, but rather there is a continuum of the diversity of orientations found in the local region surrounding any point in the map. In order to relate the tuning of responses more directly to the local orientation map structure, we characterized the selectivity of the orientation representation surrounding each recording site. We reasoned that if local connections contribute a significant portion of the synaptic drive to V1 neurons, the differences in the membrane potential responses of our neurons might be traced to differences in the orientation representation within their local circuit. Although it has been demonstrated that inhibitory inputs are strong in V1 neurons Borg-Graham et al. 1998 and Hirsch et al. 1998, studies of the orientation tuning of synaptic conductances indicate that membrane potential recordings provide a reasonable estimate of the orientation tuning of synaptic inputs (Anderson et al., 2000; see also below). Based on anatomical tracer injection studies of local synaptic connectivity Malach et al. 1993, Bosking et al. 1997, Kisvarday et al. 1997 and Yousef et al. 2001, we estimated that a circular region of radius 400 μm would provide the majority of potential local inputs to a neuron. We examined whether the orientation

distribution within this “local input region” is related to the selectivity of the synaptic inputs to a neuron, as estimated by the membrane potential response, at any location in the orientation map.

For each cell, the orientation distribution of pixels in the local input region was calculated from the orientation angle map (in 22.5° bins). The dashed circles in Figure 2 and Figure 3 show the regions used in this analysis for the four cells of Figure 2 and Figure 3. We characterized these pixel distributions using the same indices (OSI and MI) that we used to characterize the tuning curves of our neurons. Figures 5A–5D show the scatter plots of these measures for the local input region against those for the firing rate and membrane potential responses. It is noteworthy that the OSI values calculated from the local map do not overlap for the populations designated as pinwheel or domain (squares and circles, respectively). There is a continuous distribution of these indices across the map (data not shown), and our two populations capture the extremes of the distribution. There is no significant correlation between the selectivity of the firing rate and the selectivity of the local input region, as assessed by either of the measures (Figures 5C and 5D). Thus, the local map structure is a poor indicator of the selectivity of spike responses. However, there is a significant correlation between the OSI and MI values of the membrane potential responses and of the local input region (Figures 5A and 5B), indicating that the orientation representation in the local cortical network is related to the selectivity of the membrane potential responses of a neuron at all locations in the cortex. These analyses were also performed for a local input regions with radii from 200–700 μm (data not shown); correlations were strong up to ~400 μm, above which they became less robust, indicating that the selectivity of membrane potential responses is most closely related to the structure of the *local* cortical map.

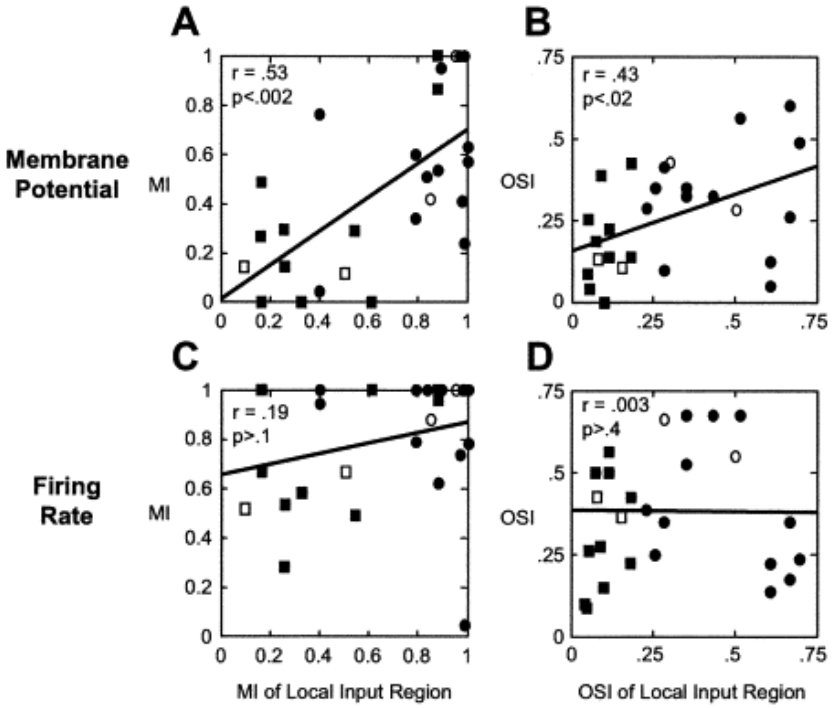

Figure 5. Local Map Orientation Representation Correlates with the Selectivity of Membrane Potential Responses but Not Spike Responses

(A) Scatter plot of the MI values of the membrane potential responses and the MI values of the local input region for each recording site. Squares indicate recording sites at pinwheels while circles indicate sites at orientation domains. Open points represent the cells shown in Figure 2 and Figure 3. Lines in this and all plots indicate the least-squares linear fit to the data. Correlation coefficients and associated p values are indicated.

(B) Scatter plot of the OSI values of the membrane potential response and the local input region of the map.

(C and D) Scatter plots of the MI and OSI values of the spike responses and the local input region.

This result provides support for the validity of our measures, the local input region and the membrane potential response, as estimates of the local synaptic pool and the activated synaptic inputs, respectively. To further assess our attribution of the source of the membrane potential responses to synaptic inputs, in a subset of our cells, we made additional recordings in the presence of constant current injections. By depolarizing or hyperpolarizing the neurons, we altered the currents through postsynaptic channels by altering the driving forces and thus obtained an estimate of the net synaptic inputs underlying the postsynaptic potentials we recorded. Figure 6 shows two examples of this analysis. Figure 6A shows a complex cell recorded in an orientation domain with three levels of current injection. The left column shows the responses to the preferred orientation, and the column to the right shows the responses to the orthogonal orientation. This example demonstrates that the neuron receives substantial synaptic input for the preferred orientation, but no discernable inputs, regardless of our manipulation of the driving forces, for the orthogonal orientation. Thus, in the case of this orientation domain neuron, the membrane potential recording at the resting potential (no current injection) provides a reasonable estimate of the net synaptic inputs the neuron receives. The example in Figure 6B, of a complex cell recorded at a pinwheel, is decidedly different. At resting potential, the neuron shows a substantial depolarization in the orthogonal condition, similar to that seen in the cells of Figure 3. However, when the neuron is depolarized, it shows a robust hyperpolarization in response to the same stimulus. This suggests that in the resting condition, the membrane potential response to the orthogonal orientation is a composite response, resulting from both excitatory and inhibitory synaptic inputs. Thus, the results from this analysis support the major result from the previous analysis of membrane potential tuning curves: neurons close to pinwheel centers receive synaptic inputs at all stimulus orientations, whereas neurons far from pinwheel centers only receive synaptic inputs over a narrow range of orientations.

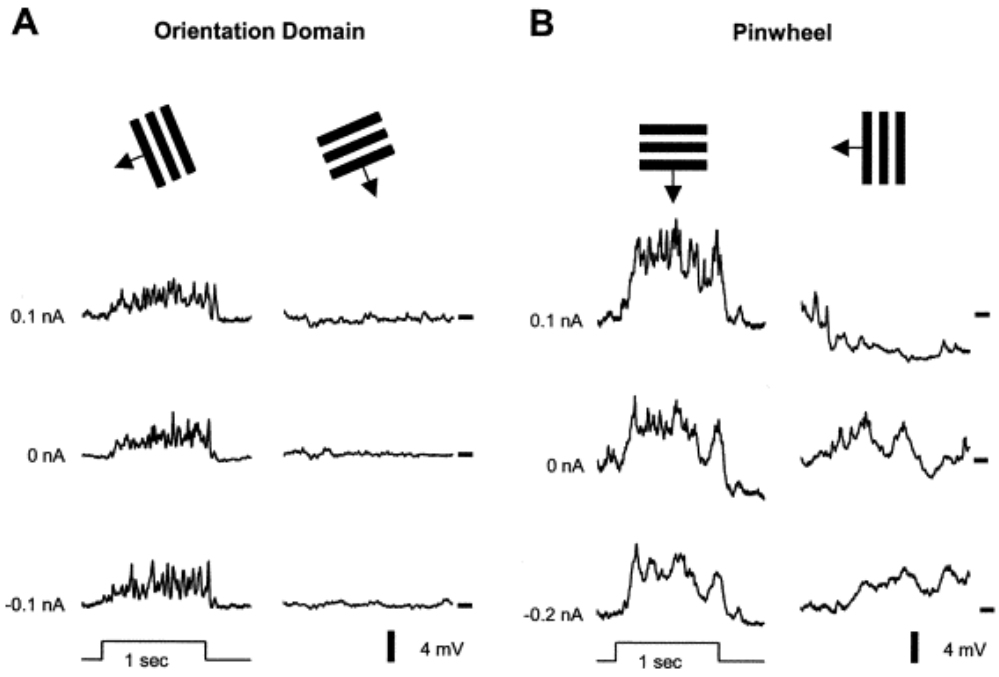

Figure 6. Synaptic Activity at Orthogonal Orientations in Pinwheel Neurons but Not Orientation Domain Neurons
(A) Responses to the preferred orientation (left column) and orthogonal orientation (right column) for a neuron located in an orientation domain. The three rows show data from identical stimuli in the presence of three levels of current injection (indicated to the left of each row) used to depolarize and hyperpolarize the cell. Regardless of the injected current, the preferred stimulus induces a robust depolarization, but the orthogonal stimulus induces no detectable membrane voltage deflection. The schematic visual gratings at the top of each column represent the stimulus orientation and direction of motion. The step function below the left column of traces depicts the time course of the stimulus. Dash marks next to the right column of traces show baseline potentials.
(B) Responses to the preferred orientation (left column) and orthogonal orientation (right column) for a neuron situated near a pinwheel center. All conventions are as in (A). This neuron shows robust depolarization in response to the preferred orientation. However, the orthogonal orientation induces a depolarization at resting or hyperpolarized potentials, but a hyperpolarization at the depolarized potential.

Discussion

Our data indicate that the orientation specificity of inputs to V1 neurons correlates with the orientation specificity of the surrounding local cortical network; however, the different patterns of input are transformed differently, such that the selectivity of spike responses is similar, regardless of map location. This result demonstrates that the input-output transformation performed by neurons in V1 is powerfully influenced by the orientation representation in their local neighborhood and hence by their location in the orientation map. We interpret this inhomogeneity in the selectivity of inputs to result from the inhomogeneity in the orientation composition of the local cortical neighborhood. It could, in principle, arise from an inhomogeneity in the inputs arising from any source. However, in light of data suggesting that the local connections are less orientation specific near pinwheel centers (Yousef et al., 2001) and absent any evidence for inhomogeneity in the thalamocortical projection, we prefer the cortical interpretation of our data. Furthermore, the fact that the selectivity of inputs correlates well with the selectivity in the local cortical representation argues strongly for the local cortical connections as the source of the difference in inputs between pinwheel and orientation domain locations.

Possible Explanations of Differences in Synaptic Integration

It is clear from a comparison of Figures 4A and 4B that neurons near pinwheel centers undergo a more severe sharpening in the transformation of subthreshold responses to spike responses. The central portion of the membrane potential tuning curves (the “tip of the iceberg”) is similar between pinwheel and orientation domain neurons, and this is the portion of the tuning curves which is translated into spikes. It is the flanks of the membrane potential tuning curves, which lie below the spike threshold, that are different between pinwheel and orientation domain neurons.

An important question that naturally arises is why the flanks of the membrane tuning curves at pinwheels are elevated compared to those of orientation domain neurons, and how they are kept below threshold and thus removed from the spike tuning curves. A simple explanation of the relationship between the selectivity of the synaptic inputs and the map representation is that neurons sum inputs from the local network in a relatively linear fashion; the area of cortex representing a particular orientation that lies within the local integration range of a neuron will determine the magnitude of the membrane potential response to that orientation. However, for several reasons, it is unlikely that V1 neurons integrate inputs entirely linearly. First, a look at our data reveals that the absolute magnitude of the maximum response is not different between pinwheel and orientation domain neurons (9.4 ± 1.9mV versus 8.3 ± 0.9mV), as would be expected if responses of neurons were linearly related to the area of cortex activated by the stimulus. If neurons were linearly summing local inputs, we would expect the depolarization in response to the preferred orientation to be much larger for orientation domain neurons, because the amount of cortex representing that orientation is much larger than for neurons near pinwheel centers. Furthermore the total response, integrated across orientation, is ~50% larger for pinwheel neurons (data not shown). This is again inconsistent with the linear interpretation, because the absolute area of the local input region is, by definition, identical.

A more fundamental reason to doubt this simple linear relationship is that V1 neurons receive large amounts of inhibition (both hyperpolarizing and shunting), which can effectively cancel or mask excitatory inputs Borg-Graham et al. 1998 and Hirsch et al. 1998. One possibility is that in pinwheel neurons, inhibition is crucial to keeping responses to nonoptimal orientations below threshold. Indeed, a recent computational model suggests that the role of inhibition in shaping the response of V1 neurons may differ as a function of distance from pinwheel centers (Wielaard et al., 2001). The examples in Figure 6 suggest that there may indeed be strong inhibitory inputs at nonpreferred orientations in neurons close to pinwheel centers. Further experiments will be necessary to quantitatively measure the excitatory and inhibitory components of visual responses and to test a more sophisticated model of inputs (both excitatory and inhibitory) than our simple circle of excitation.

The spike threshold is another nonlinearity which influences the input-output transformation performed by neurons. Indeed, previous studies have shown diversity in the magnitude of sharpening caused by the spike threshold Carandini and Ferster 2000 and Volgushev et al. 2000. We have not examined whether the spike threshold varies across the orientation map, but our data indicate that even a constant spike threshold can lead to diversity in the degree of orientation sharpening as a function of position in the orientation map. A possibility that bears careful examination is whether the threshold also varies with map location and thus dynamically regulates the portion of the tuning curve which leads to spikes (cf. Azouz and Gray, 2000).

It is also possible that the responses to near-optimal orientations are preferentially amplified by cortical processing, as has been proposed in network models of the generation of selectivity Douglas et al.

1995, Somers et al. 1995 and Somers et al. 2001. Notably, orientation-selective enhancement of spike generation (Volgushev et al., 2002) may contribute more heavily to selectivity near pinwheel centers. Thus, several possible mechanisms could account for the tuning curves we observe.

Integration of Local Inputs and Orientation Selectivity

Although our experiments do not directly address the generation of orientation selectivity in first-order thalamic-recipient cells, it is noteworthy that our major result holds for both simple and complex cells. In this respect, our results do not discriminate between models of the mechanism for the initial generation of orientation selectivity in first-order thalamic-recipient V1 neurons. However, the majority of the response of simple cells (Ferster et al., 1996) and the propagation of orientation selectivity to complex cells Alonso and Martinez 1998, Chance et al. 1999 and Martinez and Alonso 2001 depend on intracortical connections. Regardless of the mechanism that confers the initial selectivity, cortical inputs must ultimately play an important role in shaping the responses of all V1 neurons. A recent report suggests that intracortical inputs may have different roles in producing orientation selectivity at different stages (layers) of the cortical microcircuit (Martinez et al., 2002). Our data are sampled from all cortical depths, but we did not label our cells, so the laminar positions are unknown. Future studies will be required to examine any interaction between laminar location and position with regard to the orientation map. That issue aside, our data suggest that the local cortical inputs have potentially different orientation compositions at different locations in the map, and the mechanisms that ultimately shape orientation selective spike responses may be different as well. Specifically, responses to nonpreferred orientations are large, but remain subthreshold, in neurons near pinwheel centers.

A number of experiments have demonstrated that manipulation of the cortical network can reveal these subthreshold inputs. For example, it has been shown that short-term shifts in the preferred orientation induced by pattern adaptation are much more prominent near pinwheel centers (Dragoi et al., 2001). This is presumably allowed by the strong subthreshold inputs, which we show here to be much closer to threshold near pinwheel centers. It has also been shown that the selectivity of a neuron can be reduced by local inactivation of a cortical site ∼500 μm away if the orientation preference of the inactivation site is orthogonal to that of the recorded cell, but not if the inactivation site is iso-oriented with the recorded cell (Crook et al., 1997). Although these recordings were done without knowledge of the orientation map location, it is likely that sites at which an orthogonal domain is located within 500 μm will be rather near a pinwheel center. These results, together with those presented here, imply strongly that orientation selectivity is actively, and dynamically, maintained through a balance of the magnitudes of the inputs at nonpreferred orientations relative to the spike threshold. This balancing act is particularly important, and particularly susceptible to alteration of inputs, for neurons at or near pinwheel centers.

Experimental Procedures

Animal Preparation

Experiments were performed on adult cats (2–3 kg) of either sex according to procedures that were approved by MIT's Animal Care and Use Committee and conformed to NIH guidelines. Animals were prepared for imaging and recording according to procedures that have been described Rao et al. 1997 and Dragoi et al. 2000. Briefly, animals were anesthetized (1%–1.5% isofluorane in 70:30 N_2O and O_2), paralyzed with vercuronium bromide (0.2 mg/kg/hr) in a 50/50 mixture of lactated Ringer's solution and 5% dextrose, and artificially respired. Expired CO_2 was maintained at 4%; anesthesia was monitored continuously. A craniotomy and durotomy were performed over area 17, and a stainless steel chamber was mounted on the skull. The chamber was filled with agar (∼2.0% in saline), covered with a circular coverglass, and coated with viscous silicone oil.

Physiological Recordings

An orientation map was first obtained by optical imaging of intrinsic signals. Full-field, high-contrast square-wave gratings (0.5 cycle/°, 2 cycles/s) of four orientations, drifting in each of two directions, were presented using STIM (courtesy of Kaare Christian, Rockefeller University) on a 17 inch CRT monitor placed at a viewing distance of 30 cm. Images were obtained using a slow-scan video camera, (Bischke CCD-5024, Japan) equipped with a tandem macro-lens arrangement, and fed into a differential amplifier (Imager 2001, Optical Imaging, Mountainside, NJ). The cortex was illuminated with 604 nm light, and the focus was adjusted to ∼500 μm below the cortical surface during imaging. Care was taken to obtain

reference images of the surface vasculature several times over the course of the imaging session to detect any shift of the cortex relative to the camera and to increase the accuracy of electrode penetrations.

Intracellular whole-cell recordings were subsequently obtained at locations that were aligned to the angle map by reference to images of the surface vasculature. A bilateral pneumothorax was performed and a canula inserted into the cisterna magna to minimize brain movement. Patch pipettes (tip diameter ~2 μm; 12–20 MΩ) containing 120.0 mM Kglu, 5.0 mM NaCl, 2.0 mM ATP, 0.2 mM GTP, 40.0 mM HEPES, 11.0 mM EGTA, 1.0 mM CaCl, and 1.0 mM MgCl were lowered into the cortex at sites specifically targeted to pinwheel centers and to orientation domains (locations intermediate between pinwheel centers). Tight seals were obtained by gentle suction, and intracellular access was gained by increased suction and slight vibration of the pipette tip. Recordings were made in bridge mode with manual bridge balance and capacitance neutralization. Signals were amplified, digitized at 6–8 kHz (Axoclamp 2A, Axon Instruments, Union City, CA), and stored to disk on a computer running Pclamp software (Axon Instruments). Analysis was performed with custom routines written in Matlab (Mathworks, Natick, MA). Data acquisition and visual stimulus computers were synchronized by a master computer running CORTEX (NIH). Stimuli were drifting full-field, high-contrast, square-wave gratings (0.3–0.7 cycles/°, 2–5 cycles/s) of eight orientations generated by a computer running STIM and presented on a 17 inch CRT monitor at a distance of 30 cm. Each stimulus was presented 5–7 times for 1–2 s. Trials with a blank screen of uniform intermediate gray were also randomly interleaved to provide an estimate of unstimulated, background activity levels. Neurons were accepted for analysis if they had action potentials that were at least 15mV in amplitude and showed stable resting membrane potentials for a duration of recording adequate for five trials of each stimulus orientation.

Analysis

Single-condition maps were obtained by dividing the summed activity maps of each orientation by the "cocktail blank." Smoothed single condition maps were summed vectorially to produce orientation angle maps. Orientation angle maps were further smoothed for display purposes only.

Spikes were identified and extracted from membrane potential traces by setting a threshold for the first derivative (slope) of the trace, counting the time of crosses as spike times, and linearly interpolating between the points surrounding the spike waveform. Membrane potential and firing rate responses were taken as the mean response over the first second of stimulus presentation, after subtraction of baseline levels. Cells were classified as simple or complex based on the F1/F0 ratio of the spiking responses to drifting gratings (Skottun et al., 1991). To facilitate more ready comparison with the orientation angle map data, which does not include direction information, only the responses to the optimal direction were analyzed. The OSI was calculated as Swindale 1998 and Dragoi et al. 2000:

$$OSI = \sqrt{\left(\sum_{i=1}^{n} R(\theta_i)\cos(2\theta_i)\right)^2 + \left(\sum_{i=1}^{n} R(\theta_i)\sin(2\theta_i)\right)^2} \Big/ \sum_{i=1}^{n} R_i$$

where R is average response during grating presentation, and θ is orientation from 0° to 157.5°, indexed by i = 1 to 8. It is a continuous measure with values ranging from 0 (unselective) to 1 (perfectly selective). The *MI* was calculated as a measure of the relative response to the optimal orientation and the orientation orthogonal to it: $MI = (R_{opt} - R_{orth})/R_{opt}$. It is identical to the selectivity index used by others (eg., Volgushev et al., 2000), but we chose not to use this nomenclature to avoid confusion with the *OSI*. The half-width at half height was calculated as in Carandini and Ferster (2000) by fitting a gaussian function to the tuning curve data. The *OSI* and *MI* values were calculated by the same formulas on the distributions of pixels found in the local input region for the analysis in Figure 5. All measures were computed using the mean response values. Statistical comparisons of distributions of these measures were made with the Student's t test. Membrane potential traces were smoothed for display purposes only; all analysis was performed on unsmoothed traces.

Acknowledgements

We thank Casto Rivadulla, Valentin Dragoi, Alvin Lyckman, and Brandon Farley for their comments on previous versions of this manuscript, Carsten Hohnke for providing his Matlab analysis toolbox, and Christine Waite for assistance with the manuscript. This work was supported by a predoctoral fellowship from the Howard Hughes Medical Institute (J.S.), a fellowship from MECD, Spain (J.M.), and grants from the NIH (M.S.).

References

Alonso and Martinez 1998. J.M. Alonso, L.M. Martinez. Functional connectivity between simple cells and complex cells in cat striate cortex. Nat. Neurosci., 1 (1998), pp. 395–403

Anderson et al. 2000a. J.S. Anderson, M. Carandini, D. Ferster. Orientation tuning of input conductance, excitation, and inhibition in cat primary visual cortex. J. Neurophysiol., 84 (2000), pp. 909–926 a

Anderson et al. 2000b. J.S. Anderson, I. Lampl, D.C. Gillespie, D. Ferster. The contribution of noise to contrast invariance of orientation tuning in cat visual cortex. Science, 290 (2000), pp. 1968–1972 b

Azouz and Gray 2000. R. Azouz, C.M. Gray. Dynamic spike threshold reveals a mechanism for synaptic coincidence detection in cortical neurons in vivo. Proc. Natl. Acad. Sci. USA, 97 (2000), pp. 8110–8115

Blasdel 1992. G.G. Blasdel. Orientation selectivity, preference, and continuity in monkey striate cortex. J. Neurosci., 12 (1992), pp. 3139–3161

Bonhoeffer and Grinvald 1991. T. Bonhoeffer, A. Grinvald. Iso-orientation domains in cat visual cortex are arranged in pinwheel-like patterns. Nature, 353 (1991), pp. 429–431

Borg-Graham et al. 1998. L.J. Borg-Graham, C. Monier, Y. Fregnac. Visual input evokes transient and strong shunting inhibition in visual cortical neurons. Nature, 393 (1998), pp. 369–373

Bosking et al. 1997. W.H. Bosking, Y. Zhang, B. Schofield, D. Fitzpatrick. Orientation selectivity and the arrangement of horizontal connections in tree shrew striate cortex. J. Neurosci., 17 (1997), pp. 2112–2127

Carandini and Ferster 2000. M. Carandini, D. Ferster. Membrane potential and firing rate in cat primary visual cortex. J. Neurosci., 20 (2000), pp. 470–484

Chance et al. 1999. F.S. Chance, S.B. Nelson, L.F. Abbott. Complex cells as cortically amplified simple cells. Nat. Neurosci., 2 (1999), pp. 277–282

Chapman et al. 1991. B. Chapman, K.R. Zahs, M.P. Stryker. Relation of cortical cell orientation selectivity to alignment of receptive fields of the geniculocortical afferents that arborize within a single orientation column in ferret visual cortex. J. Neurosci., 11 (1991), pp. 1347–1358

Crook et al. 1991. J.M. Crook, U.T. Eysel, H.F. Machemer. Influence of GABA-induced remote inactivation on the orientation tuning of cells in area 18 of feline visual cortex: a comparison with area 17. Neuroscience, 40 (1991), pp. 1–12

Crook et al. 1997. J.M. Crook, Z.F. Kisvarday, U.T. Eysel. GABA-induced inactivation of functionally characterized sites in cat striate cortex: effects on orientation tuning and direction selectivity. Vis. Neurosci., 14 (1997), pp. 141–158

Das and Gilbert 1999. A. Das, C.D. Gilbert. Topography of contextual modulations mediated by short-range interactions in primary visual cortex. Nature, 399 (1999), pp. 655–661

Douglas et al. 1995. R.J. Douglas, C. Koch, M. Mahowald, K.A. Martin, H.H. Suarez. Recurrent excitation in neocortical circuits. Science, 269 (1995), pp. 981–985

Dragoi et al. 2000. V. Dragoi, J. Sharma, M. Sur. Adaptation-induced plasticity of orientation tuning in adult visual cortex. Neuron, 28 (2000), pp. 287–298

Dragoi et al. 2001. V. Dragoi, C. Rivadulla, M. Sur. Foci of orientation plasticity in visual cortex. Nature, 411 (2001), pp. 80–86

Ferster 1986. D. Ferster. Orientation selectivity of synaptic potentials in neurons of cat primary visual cortex. J. Neurosci., 6 (1986), pp. 1284–1301

Ferster et al. 1996. D. Ferster, S. Chung, H. Wheat. Orientation selectivity of thalamic input to simple cells of cat visual cortex. Nature, 380 (1996), pp. 249–252

Gilbert and Wiesel 1990. C.D. Gilbert, T.N. Wiesel. The influence of contextual stimuli on the orientation selectivity of cells in primary visual cortex of the cat. Vision Res., 30 (1990), pp. 1689–1701

Gillespie et al. 2001. D.C. Gillespie, I. Lampl, J.S. Anderson, D. Ferster. Dynamics of the orientation-tuned membrane potential response in cat primary visual cortex. Nat. Neurosci., 4 (2001), pp. 1014–1019

Hirsch et al. 1998. J.A. Hirsch, J.M. Alonso, R.C. Reid, L.M. Martinez. Synaptic integration in striate cortical simple cells. J. Neurosci., 18 (1998), pp. 9517–9528

Hubel and Wiesel 1962. D.H. Hubel, T.H. Wiesel. Receptive fields, binocular interaction and functional architecture of the cat's visual cortex. J. Physiol., 160 (1962), pp. 106–154

Kisvarday et al. 1997. Z.F. Kisvarday, E. Toth, M. Rausch, U.T. Eysel. Orientation-specific relationship between populations of excitatory and inhibitory lateral connections in the visual cortex of the cat. Cereb. Cortex, 7 (1997), pp. 605–618

Knierim and van Essen 1992. J.J. Knierim, D.C. van Essen. Neuronal responses to static texture patterns in area V1 of the alert macaque monkey. J. Neurophysiol., 67 (1992), pp. 961–980

Lampl et al. 2001. I. Lampl, J.S. Anderson, D.C. Gillespie, D. Ferster. Prediction of orientation selectivity from receptive field architecture in simple cells of cat visual cortex. Neuron, 30 (2001), pp. 263–274

Levitt and Lund 1997. J.B. Levitt, J.S. Lund. Contrast dependence of contextual effects in primate visual cortex. Nature, 387 (1997), pp. 73–76

Malach et al. 1993. R. Malach, Y. Amir, M. Harel, A. Grinvald. Relationship between intrinsic connections and functional architecture revealed by optical imaging and in vivo targeted biocytin injections in primate striate cortex. Proc. Natl. Acad. Sci. USA, 90 (1993), pp. 10469–10473

Maldonado et al. 1997. P.E. Maldonado, I. Godecke, C.M. Gray, T. Bonhoeffer. Orientation selectivity in pinwheel centers in cat striate cortex. Science, 276 (1997), pp. 1551–1555

Martinez and Alonso 2001. L.M. Martinez, J.M. Alonso. Construction of complex receptive fields in cat primary visual cortex. Neuron, 32 (2001), pp. 515–525

Martinez et al. 2002. L.M. Martinez, J.M. Alonso, R.C. Reid, J.A. Hirsch. Laminar processing of stimulus orientation in cat visual cortex. J. Physiol., 540 (2002), pp. 321–333

McLaughlin et al. 2000. D. McLaughlin, R. Shapley, M. Shelley, D.J. Wielaard. A neuronal network model of macaque primary visual cortex (V1): orientation selectivity and dynamics in the input layer 4Calpha. Proc. Natl. Acad. Sci. USA, 97 (2000), pp. 8087–8092

Movshon et al. 1978. J.A. Movshon, I.D. Thompson, D.J. Tolhurst. Spatial summation in the receptive fields of simple cells in the cat's striate cortex. J. Physiol., 283 (1978), pp. 53–77

Rao et al. 1997. S.C. Rao, L.J. Toth, M. Sur. Optically imaged maps of orientation preference in primary visual cortex of cats and ferrets. J. Comp. Neurol., 387 (1997), pp. 358–370

Reid and Alonso 1995. R.C. Reid, J.M. Alonso. Specificity of monosynaptic connections from thalamus to visual cortex. Nature, 378 (1995), pp. 281–284

Ringach et al. 1997. D.L. Ringach, M.J. Hawken, R. Shapley. Dynamics of orientation tuning in macaque primary visual cortex. Nature, 387 (1997), pp. 281–284

Ringach et al. 2002. D.L. Ringach, C.E. Bredfeldt, R.M. Shapley, M.J. Hawken. Suppression of neural responses to nonoptimal stimuli correlates with tuning selectivity in macaque v1. J. Neurophysiol., 87 (2002), pp. 1018–1027

Schuett et al. 2001. S. Schuett, T. Bonhoeffer, M. Hubener. Pairing-induced changes of orientation maps in cat visual cortex. Neuron, 32 (2001), pp. 325–337

Skottun et al. 1991. B.C. Skottun, R.L. De Valois, D.H. Grosof, J.A. Movshon, D.G. Albrecht, A.B. Bonds. Classifying simple and complex cells on the basis of response modulation. Vision Res., 31 (1991), pp. 1079–1086

Somers et al. 1995. D.C. Somers, S.B. Nelson, M. Sur. An emergent model of orientation selectivity in cat visual cortical simple cells. J. Neurosci., 15 (1995), pp. 5448–5465

Somers et al. 2001. D. Somers, V. Dragoi, M. Sur. Orientation selectivity and its modulation by local and long-range connections in visual cortex. B.R. Payne, A. Peters (Eds.), The Cat Primary Visual Cortex, Academic Press, Boston (2001) 471–520.pp

Swindale 1998. N.V. Swindale. Orientation tuning curves: empirical description and estimation of parameters. Biol. Cybern., 78 (1998), pp. 45–56

Toth et al. 1997. L.J. Toth, D.S. Kim, S.C. Rao, M. Sur. Integration of local inputs in visual cortex. Cereb. Cortex, 7 (1997), pp. 703–710

Volgushev et al. 1993. M. Volgushev, X. Pei, T.R. Vidyasagar, O.D. Creutzfeldt. Excitation and inhibition in orientation selectivity of cat visual cortex neurons revealed by whole-cell recordings in vivo. Vis. Neurosci., 10 (1993), pp. 1151–1155

Volgushev et al. 1995. M. Volgushev, T.R. Vidyasagar, X. Pei. Dynamics of the orientation tuning of postsynaptic potentials in the cat visual cortex. Vis. Neurosci., 12 (1995), pp. 621–628

Volgushev et al. 2000. M. Volgushev, J. Pernberg, U.T. Eysel. Comparison of the selectivity of postsynaptic potentials and spike responses in cat visual cortex. Eur. J. Neurosci., 12 (2000), pp. 257–263

Volgushev et al. 2002. M. Volgushev, J. Pernberg, U.T. Eysel. A novel mechanism of response selectivity of neurons in cat visual cortex. J. Physiol., 540 (2002), pp. 307–320

Wielaard et al. 2001. D.J. Wielaard, M. Shelley, D. McLaughlin, R. Shapley. How simple cells are made in a nonlinear network model of the visual cortex. J. Neurosci., 21 (2001), pp. 5203–5211

Yao and Dan 2001. H. Yao, Y. Dan. Stimulus timing-dependent plasticity in cortical processing of orientation. Neuron, 32 (2001), pp. 315–323

Yousef et al. 2001. T. Yousef, E. Toth, M. Rausch, U.T. Eysel, Z.F. Kisvarday. Topography of orientation centre connections in the primary visual cortex of the cat. Neuroreport, 12 (2001), pp. 1693–1699